Experimentation and Application of Differential Inductive System for Machine and Human Body Parametric Measurement

Abdulwahab Deji[1], Sheroz Khan[2], Musse Mohamoud Ahmad[3]

[1]Department of Electrical Computer Information and Telecommunication Engineering, Waidsum University Malaysia.
[2]Department of Electrical Engineering Onaizah College Saudi Arabia.
[3]Department of Electrical and Computer Engineering University of Malaysia Sarawak.

Abstract

In this article, the prototype circuit is constructed and tested to confirm the results obtained through simulation of a differential inductive circuitry. However, some number of errors found are reported in section 7. Analysis is done between the experimentally found results and those obtained from simulation. Test is done on all sections and certain test parameters are set to determine the actual performance of the system. The test parameters are the frequency response of the differential inductive circuit, the oscillatory effect of the movement of the core in and out of the coil, the inductance change, the force/pressure providing motion, wind pressure, the speed of the inward movement of the core and that of the outward movement, the number of turns used, the length of coils, the area of the coil topology, the diameter of the coil and that of the core, the mass of the convulsion bar, the mass of the target, the ambient temperature of the surrounding, density of the magnetic material used, the applied voltage to the timer, the resonant frequency reached, the amount of current voltage and frequency generated, the percentage of the duty cycle found on the resulting signal, the frequency hysteresis found, the range of oscillation bar, the height of coil arrangement, the seesaw concept, the output waveform of the signal, amongst others. The summary of the major contribution of this work includes a novel design of a differential inductive position sensory system along with its model in the form of the sensed parameter equations as a function of the displacement along the length of the coil. The analytical model for linearization compensation and improved transducer response is another component the author of this work claims it as contribution

Keyword: Prototype circuit, experimental values, coil topology, test parameter, parametric measurement, position sensing, frequency hysteresis, power loss, ferromagnetic and non-ferromagnetic materials.

1. INTRODUCTION

The utility of this work lies in a broader data acquisition system making use of differential sensors. It has provided for a detailed design and implementation of a system that can be implemented for position sensing acquiring data from oscillation deflections in millimeter and micrometer range sensing. The method used is an alternative to the current data acquisition systems using cantilever mechanism by Ezzat 2011, Bruno 2013 and 2014.

The differential inductive sensor circuit is built around an inexpensive high performance 555 timer-based circuits, capable of processing up to eight analog inputs from various transducers into a digital output using a R3R-L model. This helps in acquiring digital data that would further been used for wireless application such as UWB signal.

The output frequency and voltage signal can be interfaced with a based board inexpensive UWB modem, for its transmission. This circuit can be used to sense a number of scenario; such as the liquid level in a tank, biomedical applications in determining the expansion and contraction of the muscles or bones for that matter, metal deposits, the amount of bend in a bimetallic strip, the expansion and contraction in roads and railways, cracks in building for civil application. Deji A., Sheroz K., Musse M.A., (December 2023) The designed differential sensor measurement unit has been proven to complement and support the study of measurement and instrumentation and could be applied in various industries for unlimited applications. It provides linkages between the data generating sensors towards any processing unit with serial interfacing capabilities. Deji A., Hanifah A.M., Sherifah O.M., (November 2023)

In the not very distant future, this system could be fitted into a personal digital assistant (PDA) or might be used in enhancing the features of a hand-held calculator or even if ultimately designed as chip, it can be fitted in human body. This can therefore read bio-signals of interests for diagnosing ailments, then sending the situation to a mobile phone for an expert opinion of a medical doctor, or even alerting the attention of an off-site doctor in cases where emergency arises. the prototype of the core-coil model is shown in Figure 1. This is to be used in other applications or to be fabricated by those who may improve on the concept of this work. Khan S., A. Deji, A.H.M Zahirul, J. Chebil, M.M Shobani, A.M Noreha. (Setember 2012)
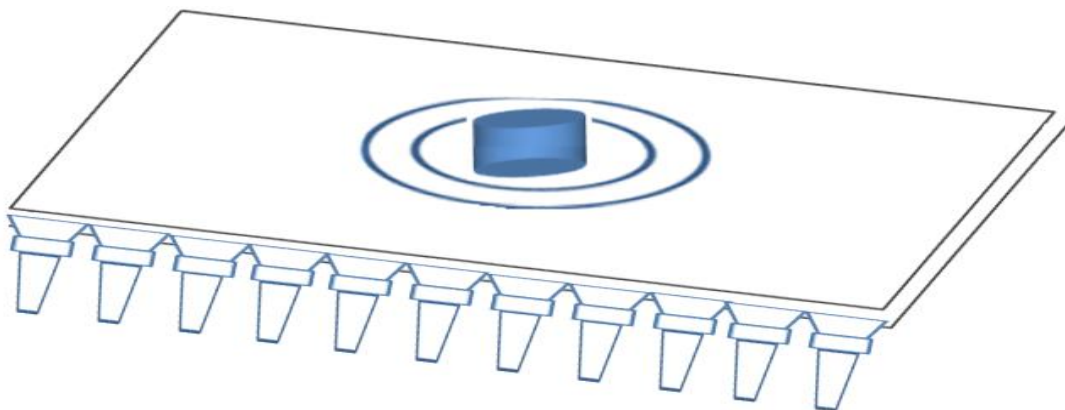

Figure 1: Prototype design for future implementation

2. Design Parameter Listing for Experimentation

This section is segmented into two parts; namely the experimental parameter and the process parameters. The experimental parameters involve the chosen parametric values used in the experiment in order to obtain the desired output. This includes but not limited only to the parameters listed in section 2.1 and 2.2.

Experimental Parameters

This section presents the experimentation aspect of the derivation results and simulation results in the previously reported work. The experimental setup of the simulated circuit of Figure 2 (a) and (b) is carried out in this section and the results obtained are presented in section 4 and beyond. The values of the parameter used are thus:

Coils (N=1000), 2 cores (aluminum and mild steel), 2 resistors of 10kΩ and 30kΩ, 555 timer, Function Generator, Power supply, 0.01µF capacitor, jumper wire, circuit board etc.

Process Parameters

For the prototype device described in this chapter, here under focus are the aforementioned parameters and physical quantities.

- The length of the core and that of the coil is 20mm
- The mass of the cores used ranges from 0.68g to 0.98g
- The total number of turns N in the coil is 100
- The radius of the coil is 1mm and its resistance is 1kΩ, giving cross sectional area of the coil used in the experiment
- The relative permeability of iron core is 4728, that of nickel is 600 and copper is 0.999834
- The displacement varies from 0.001 to 0.020m. This gives a pressure range of 0.3kPa to 12.3kPa which is the dynamic range of the developed sensor, which stays in the range of pressure by heart beat.
- The spring constant, K, is 91.33N/m
- The maximum inductance, L, obtained and the minimum was calculated $L_{min}=L_{max}/\mu_r$ for the different core material. The equations for the input and out inductance are given in equation 1 and 2 as shown:

$$L_{TOTAL} = \frac{\mu_0 N^2 A}{l}\left[\mu_r \frac{x}{l} + \frac{l-x}{l}\right] = \frac{\mu_0 N^2 A}{l}\left[1 + \frac{x}{l}(\mu_r - 1)\right] \tag{1}$$

$$L_{TOTAL} = \frac{\mu_0 N^2 A}{l}\left[\frac{x}{l} + \mu_r(\frac{l-x}{l})\right] = \frac{\mu_0 N^2 A}{l}\left[\mu_r + \frac{x}{l}(1 - \mu_r)\right] \tag{2}$$
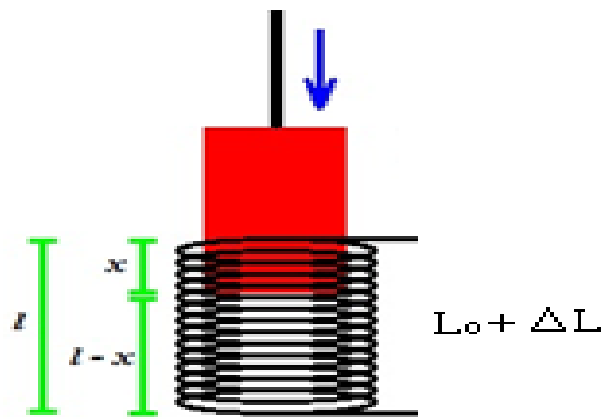
Experimental Set-Up

This work further shows and verifies that the performance of the system is evaluated in the laboratory in order to validate the simulation results in literature [Deji A., Sheroz K., Musse M.A., 2023] and [Deji A., Sheroz K., Musse M.A., 2023]. However, the experimental set-up has its own drawback and difficulties encountered during this stage. This is analyzed under sub-sections on errors, both in the output frequency and voltage of the resulting signal as seen from both simulation and experiments. The analysis shows that across the entire range of the response frequency is ultimately proportional to the parameter being sensed. D. Abdulwahab et al.

D. Abdulwahab, S. Khan, J. Chebil and A. H. M. Z. Alam (2010), Deji A., Sheroz K, Musse M.A, Jalel C. (August 2014) and Deji A., Sheroz K, Musse M.A, Jalel C. (2011)
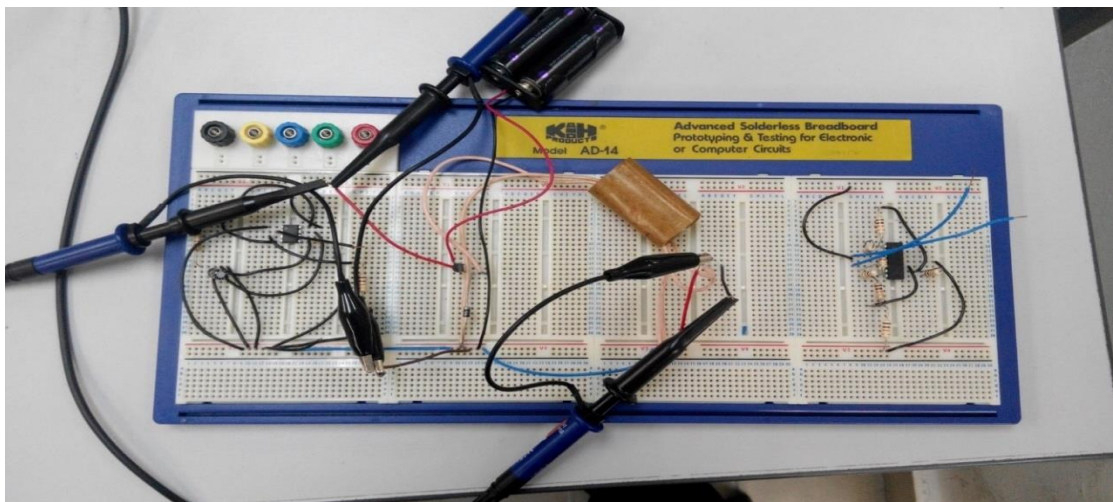
Therefore, the set-up for the various stages of experimentation is as shown in Figure. 2. Figure 2 (a) and (b) shows a system whereby the magnetic core goes in and out of the coil topology as a result of oscillation hence producing differential signal in a differential manner. While Figure 2 c shows the experimental setup.

(a)
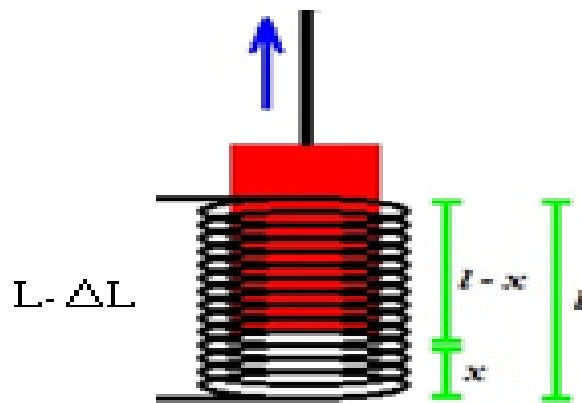
(b)

(c)

Figure 2: (a) Differential core moving into a coil due to vibrations (b) Differential core moving out of the coil due to vibrations (c) Experimental set-up for Differential Inductive Sensing
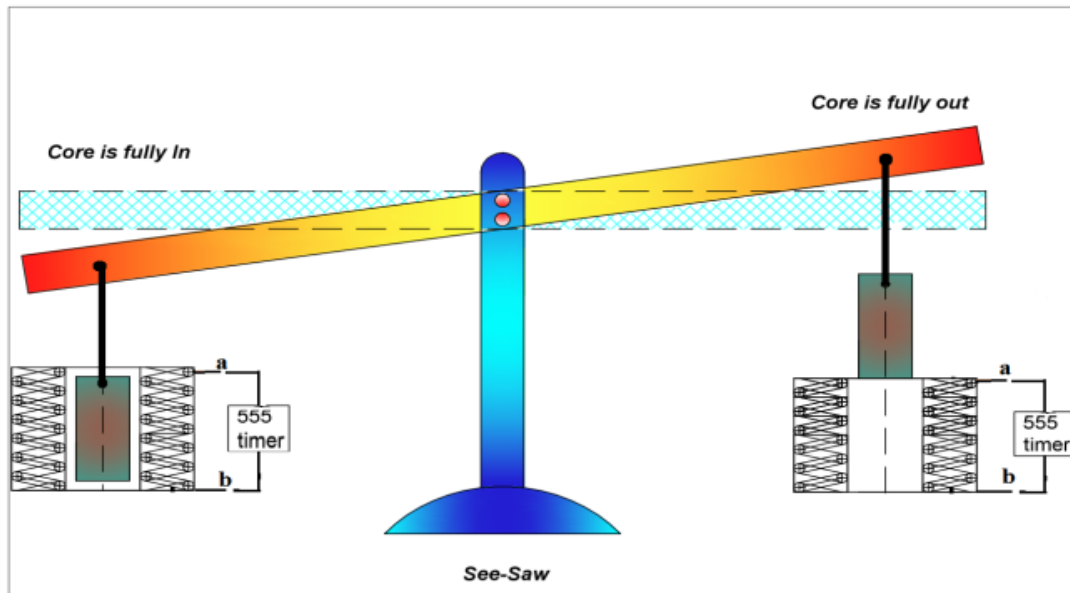
Figure 3: Differential core oscillation producing frequency.

When the core is inserted into the coils, at every length reached, the resulting frequency is measured, calculated and finally compared. Similarly, when the core is being removed from the coils, at various length, frequency is measured, calculated and compared. These are comprehensively shown in table 1, table 2, table 3 and table 4. Plots expressing the tabular results are shown in section 5.

Magnetic Core Materials Used

A magnetic core is a piece of magnetic material with a high permeability used to confine and guide magnetic fields in electrical, electromechanical and magnetic devices such as electromagnets, transformers, electric motors, generators, inductors, magnetic recording devices and other magnetic couplings. In the case of magnetic application coupling, the core could be ferromagnetic metal eg iron, or ferromagnetic compounds eg ferrites. The high permeability, relative to the surrounding air, causes the magnetic field lines to be focused into the core material. The magnetic field is often created by a coil of wire around the core that carries a current. Bruno (2013)

The use of a magnetic core can obviously make use of strength and increase the effect of magnetic fields produced by electric current. The properties of the differential position sensing device practically depend absolutely on the following factors:

- The geometry of the core material.
- The amount of air/wind gap in the designed sensor circuit.
- The characteristics of the core material, that is permeability, hysteresis etc).
- The operating temperature of the core material.
- Lamination to reduce eddy currents

In many applications it is undesirable for the core to retain magnetization when the applied field is removed. This property, called *hysteresis* can cause energy losses in applications such as transformers. Therefore 'soft' magnetic materials with low hysteresis, such as silicon steel, rather than the 'hard' magnetic materials used for permanent magnets, are usually better used as cores. This essence, is to minimize the hysteresis emanating from the model in order to give better system utility and optimization of the designed differential position sensor.

4.1 Aluminum used as Core

When aluminium is used as core, the result is shown in table 1 below. Table 1 shows the various length of the core as it is moving into the coil. This change in inductance produces a corresponding

4.2 Iron/Steel used as Core

"Soft" (iron) is used in magnetic couplings, electromagnets and in some electric motors; and it can create a useful field that is as much as 50,000 times more than an air core. This is why the air/wind force contribution in the differential is very little compared to the force applied causing significant oscillation. Iron is desirable to make magnetic cores, as it can withstand high levels of magnetic fields without saturating. It is also used because, unlike "hard" iron, it does not remain magnetized when the field is removed, which is often important in applications where the magnetic field is required to be repeated interchangeably.

Unfortunately, due to the electrical conductivity of the metal, at AC frequencies it can often suffer from large eddy currents circulating within it. This helps to waste energy and cause undesirable heating of the iron.

The result from the choice of iron as core are shown in table 3 and table 4. This is further shown in Figure 5 showing the hysteresis behavior in the inward and outward geometry of the core.

4.3 Air as Magnetic Core Material

A coil not containing a magnetic core is called an air core. This includes coils wound on a plastic or ceramic form in addition to those made of stiff wire that are self-supporting and have air inside them. Air core coils generally have a much lower inductance than similarly sized ferromagnetic core coils, but are used in radio frequency circuits to prevent energy losses called core losses that occur in magnetic cores. The absence of normal core losses permits a higher Q factor, so air core coils are used in high frequency resonant circuits, such as up to a few megahertz.

However, losses such as proximity effect and dielectric are still present. Air cores are also used when field strengths above around 2 Tesla are required as they are not subject to saturation. (Deji, A., Khan, S., Habaebi, H.M., Musa. O.S. (2024)

Again, when the iron/steel is used as the core, the frequency obtained as a result of change in the inductance is shown in table 3. The movement of the iron core with respect to the used coils into and out of the coils is shown in table 3 and table 4

Results and Discussion

An experimentation of the designed mathematical model and its necessary derivations for frequency, frequency hysteresis, for the various magnetic materials used as core and their responses are carried out. The results obtained confirm the mathematical derivation plots with the simulation. Bruno 2013, D. Abdulwahab et al. (2010), D. Abdulwahab, S. Khan, J. Chebil and A. H. M. Z. Alam (2011), Deji A., Sheroz K, Musse M.A, Jalel C. (August 2014), Deji A., Sheroz K, Musse M.A, Jalel C. (2011) and Deji A., Sheroz K, Musse M.A, (November 2023) and Deji A., Sheroz K, Musse M.A, (December (2023).

Figure 4 (a-b) is the result of the experimentation of both circuits; the right and the left one using the same assumption that was used in the calculations. Figure 5 (a-b) represents the values of the average frequency in and out of iron and aluminum core used when the magnetic core was going in, with its red representing the measured frequency and green representing the calculated frequency. Figure 5 (a-b) shows the result

of the values of the average frequency in and out of iron and aluminum with its red line showing inward frequency and green line showing its outward frequency for both iron and aluminum. The measured and calculated frequencies are plotted against the various displacement of the core as shown in Figure 6. These are also explained in table 1 and 2. Figure 4 and 5 also shows the frequency output hysteresis for the output frequency as shown by the displacement of the inward and outward movement of the of the iron and aluminum core. The frequency increases as the core is displaced from the coil arrangement. This shows that the inductance of the magnetic material is proportional to its displacement and its output response. These are also explained in table 3 and 4. Figure 6 represents the frequency against the inductance for both measured and calculated. The difference in the output value of these frequencies are as a result of the environmental condition of the devices and experimental errors, which are not found or minima in terms of derivations and simulation. A benchmarked of the results with (Ezzat 2011, Ezzat 2012, Mohammed 2012, and Ferran 2009, Sheroz 2012) and Deji 2010, Deji 2011, Deji 2012, Deji 2014, Deji 2016 Deji 2023, Deji 2023 and Deji 2024) shows a significant improvement in method of circuit connection, configurations resulting to improved output response in terms of frequency, inductance, displacement and vibrations of devices into useful signal.

Change in the frequency.

Table 1: Aluminium core going into magnetic coils

LENGTH (CORE IN)	1ST Freq	2ND Freq	3RD Freq	AVERAGE(IN) Freq
6	235.8	217.6	235.8	**229.7**
12	242.7	225.2	237.8	**235.2**
18	245.4	235.9	238.2	**239.8**
24	253.5	236.8	240.3	**243.5**
30	262.5	240.1	241.8	**248.1**
36	263.1	242.2	263.3	**256.2**

Again, as the aluminum core goes out of the design coil transducer, these results are obtained and tabulated in table 2.

Table 2: Aluminum core going out of magnetic coils

LENGTH (CM) (CORE OUT)	1ST Freq	2ND Freq	3RD Freq	AVERAGE(k), Freq (OUT)
6	210.0	218.0	233.7	**220.6**
12	236.0	235.9	235.9	**235.9**
18	237.9	237.8	236.1	**237.3**
24	238.3	238.1	238.3	**238.2**
30	240.4	240.2	240.3	**240.3**
36	263.1	242.2	263.3	**256.2**

The corresponding frequencies for the inductive change when the aluminium core is going out are shown in the table 2 above.

Table 3: Iron/steel core going into magnetic coils

LENGTH (CM) (CORE IN)	1ST Freq	2ND Freq	3RD Freq	AVERAGE(k) Freq
6	235.3	238.1	238.0	**237.1**
12	242.8	242.2	240.5	**241.8**
18	242.4	250.0	242.6	**245.0**
24	250.7	257.2	247.8	**251.9**
30	255.0	260.5	255.5	**257.0**
36	259.5	265.8	263.9	**263.1**

Table 4: Iron/steel core going out of magnetic coils

LENGTH CORE OUT	1ST Freq	2ND Freq	3RD Freq	AVERAGE(k) OUT(Freq)
6	237.8	235.6	240.3	**237.9**
12	243.0	245.0	245.1	**244.4**
18	247.6	252.4	252.3	**250.8**
24	252.4	255.5	258.0	**255.3**
30	255.3	260.6	260.1	**258.7**
36	259.5	265.8	263.9	**263.1**

A comprehensive experimental result obtained is summarized in table 5.

**Table 5: Summary of the measured and calculated frequency and their percentage error.**

L (m)	X (m)	L-X (m)	Freq Measured (k)	Freq calculated (k)	Freq calculated (k)	Percentage % error
0.036	0.000	0.036	256.2	1100	66	74
0.036	0.006	0.030	240.3	6587	394	64
0.036	0.012	0.024	238.2	3303	197	17
0.036	0.018	0.018	237.3	2200	131	45
0.036	0.024	0.012	235.9	1649	99	56
0.036	0.030	0.006	220.2	1321	79	64

The results from table 1 and 2 are shown in Figure 4(a) and (b)

Figure 4 (a) shows a comparison of the inward motion between aluminum as core and iron as core. The result shows that the frequency output produced when iron is used as core is much higher as compared to using aluminum as the magnetic core. Although, they both increases as the core is displaced more into the page (into the coil geometry) hence resulting to output frequency in the inward motion as a result of the change in the inductance in this experiment. Figure 4 (b) shows the frequency output as a result of the outward motion for both iron and aluminum. This again shows that the output frequency for iron is higher than that of the aluminum as both cores are being removed by oscillation.
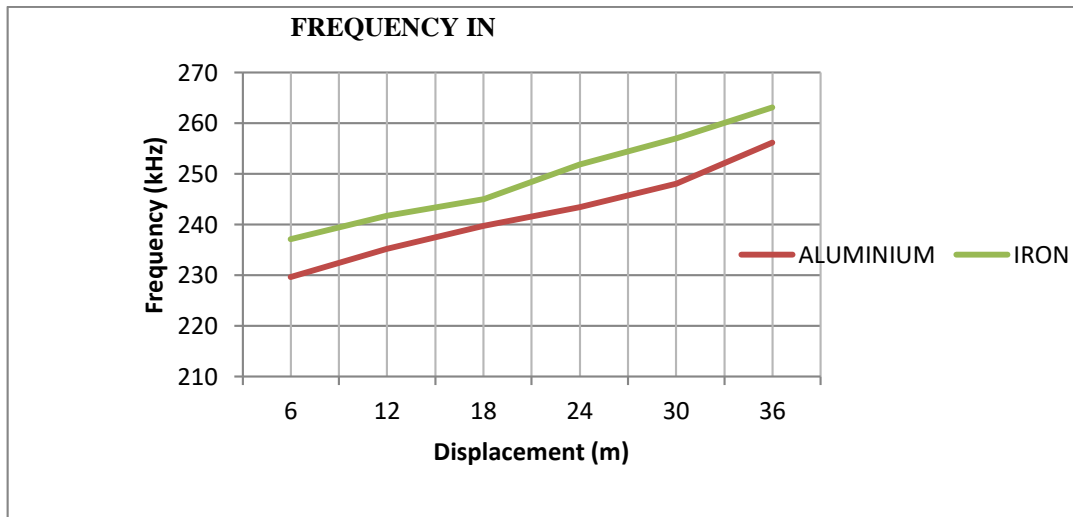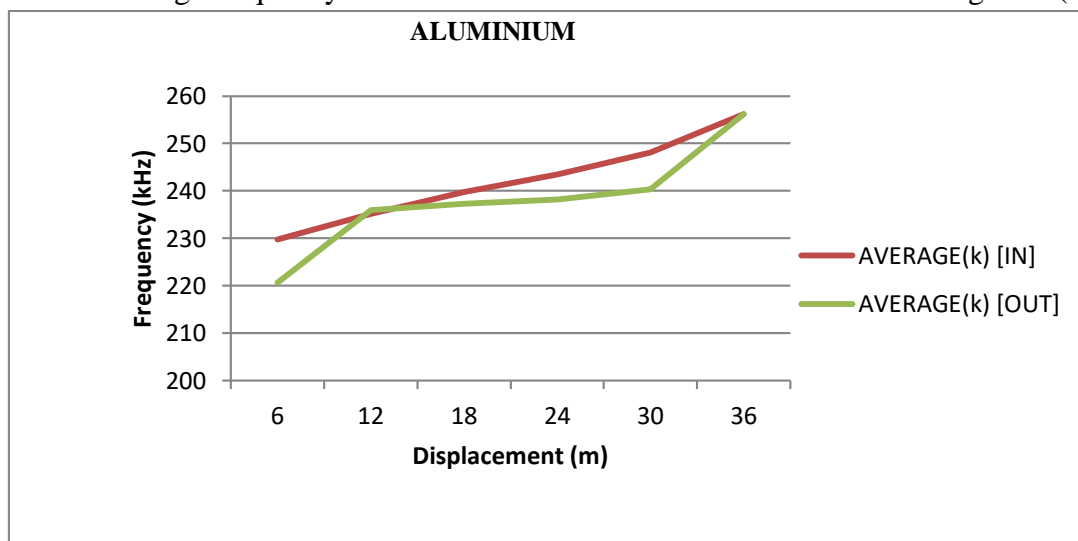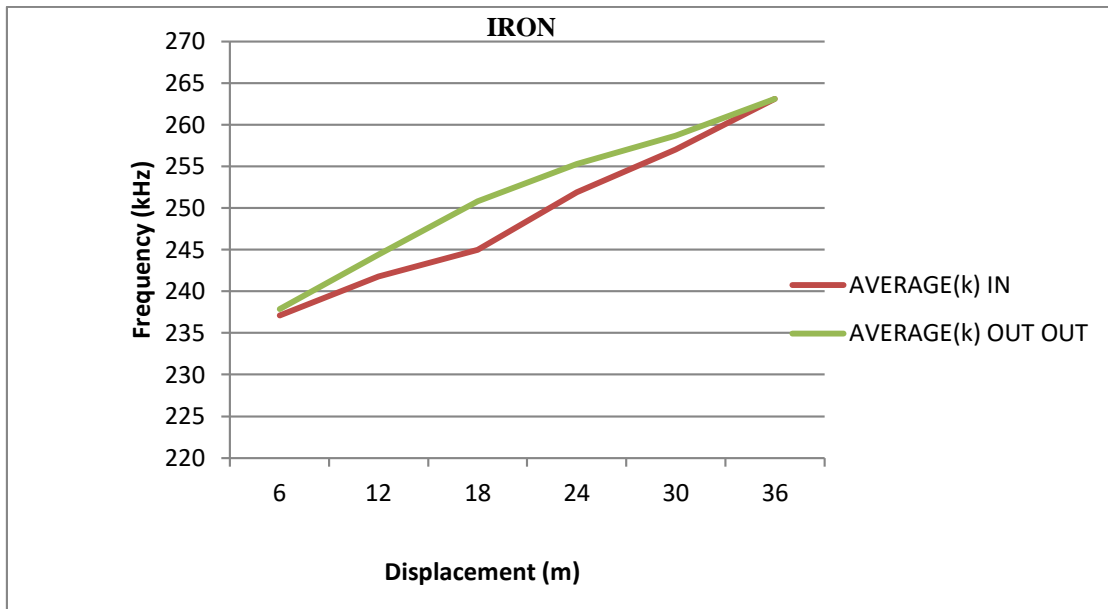
(a)
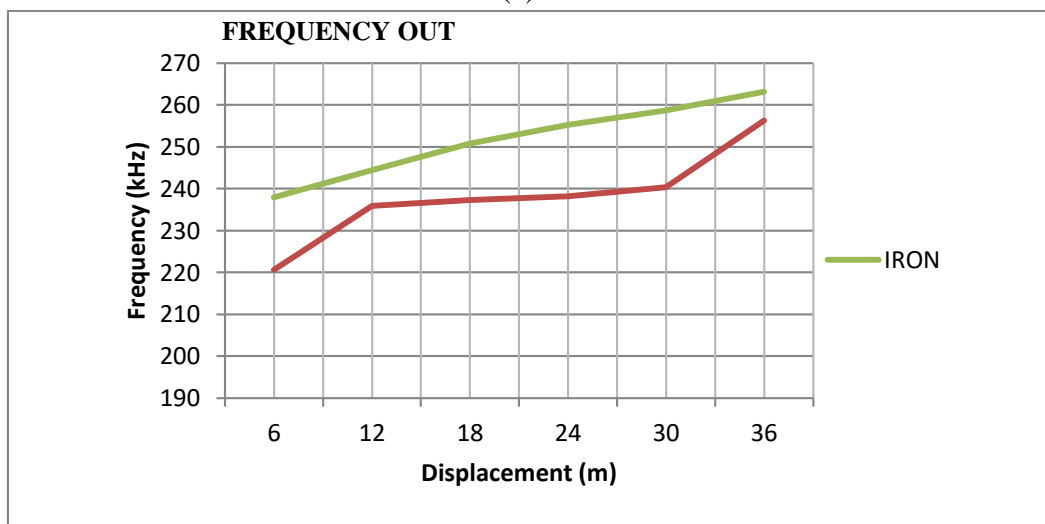
(b)

Figure 1 (a-b) Frequency value for in and out displacement for iron and aluminum core.

The values of the average frequency in and out of iron and aluminum are shown in Figure 5 (a) and (b).

(a)

(b)

Figure 2: (a-b) Frequency hysteresis for the average value for in and out displacement of the core for iron and aluminum.

Figure 5 above shows the hysteresis characterization for both aluminum and iron in both inward and outward of the core. These becomes issues that can be improved upon by minimizing the hysteresis factor to give a better system performance under high temperature and pressure under oscillation. The contribution of this article is to identify the presence of frequency hysteresis during oscillation in practical sense, that could hinder other useful output result. The frequencies calculated and measured are given in Figure 6. This shows the difference between experimentally obtained results and results from their derivations and calculation.
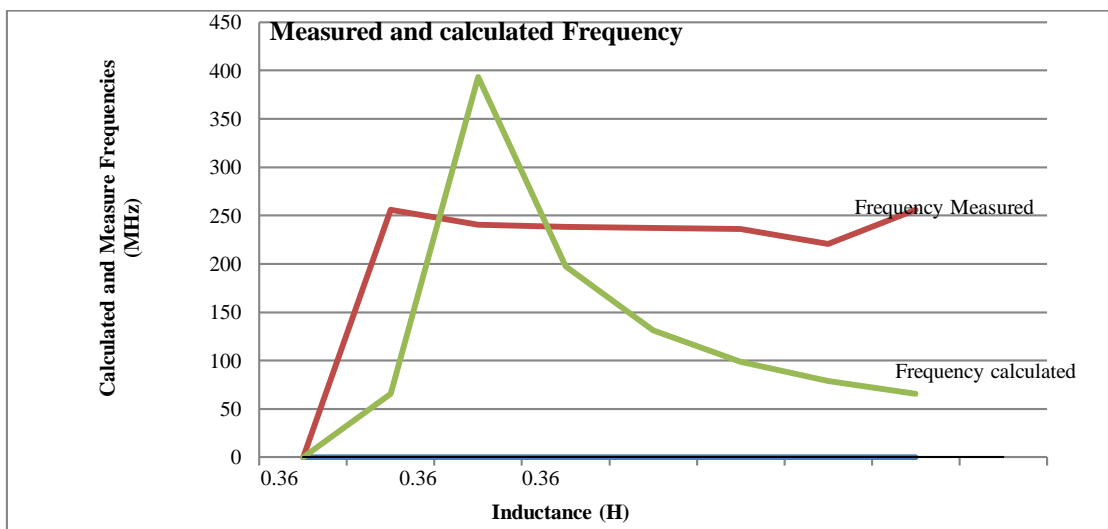

Figure Error! No text of specified style in document.**: Frequency against the inductance output from derivation and measurement.**

These frequencies show slight variation in result obtained. The difference is shown in the error section as this is so because of the surrounding factors.

3. System Losses

Core Loss

When the core is subjected to a changing magnetic field, since it's a devices that use AC current similar in principle and in use to those of transformers, inductors and AC Motors and alternators, then some of the power that would practically be transferred through the device are lost in the core, dissipated as heat and sometimes noise. The losses are often described as being in three categories:
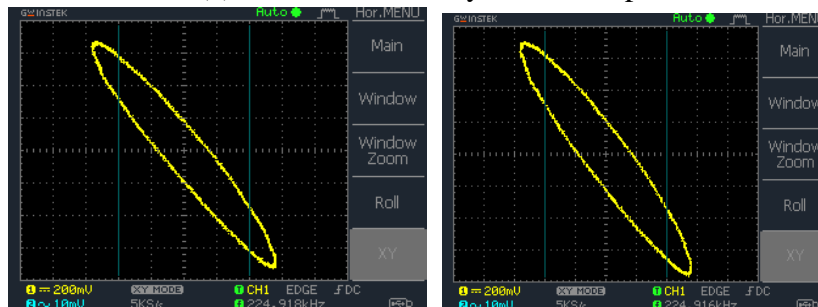
Hysteresis losses

When the magnetic field through the core changes, the magnetization of the core material changes by expansion and contraction of the tiny magnetic domains that the oscillatory system is composed of, due to movement of the domain walls. This process causes losses, because the domain walls get hot and dissipate energy as heat. This is called hysteresis loss. The amount of energy lost in the material in one cycle of the applied field is proportional to the area inside the hysteresis loop. Since the energy lost in each cycle is constant, hysteresis power losses increase proportionally with output frequency obtained.
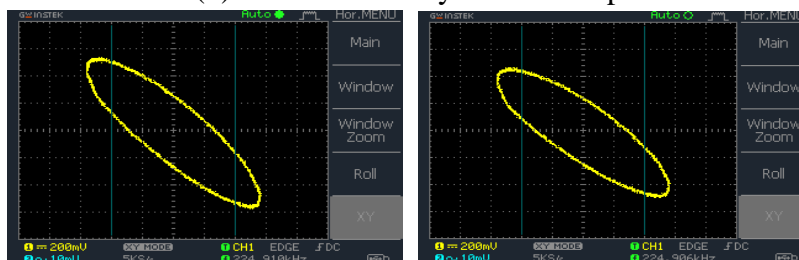
Core is half way Hysteresis (B-H)   Core is fully in Hysteresis (B-H)

(a)   Plastic core hysteresis loop

(b)   Iron core Hysteresis Loop

(c)   Steel core Hysteresis Loop

Figure 3: B-H Hysteresis curve for plastic, iron and Steel in half wave and full wave mode

In ferromagnetic and ferroelectric materials, as a result of when the input is increased and decrease sequentially, the output takes an oval shape loop which shows irreversibility. Hysteresis loops are obtained by plotting B vs. H hence it is also called B-H curve. The materials used as core will affect the size and shape of the hysteresis loop because each materials have a different relative permeability. The size of the hysteresis loops for each material are different when the core is moving through the transformer. The following table shows effect of core movement on the size (area) of hysteresis loop:

Table 6: B-H characteristics for different magnetic core materials.

Type of core material	A (mm)	B (mm)	Area (mm²)
Air core	3	27	254.47
Plastic core halfway through	3	27	254.47
Plastic core fully though	3	27	254.47
Iron core halfway through	3.75	28	329.87
Iron core fully through	4.5	29	409.98
Steel core halfway though	6	24	452.39
Steel core fully through	6	22	414.69

Eddy-current losses

If the core is electrically conductive, the changing magnetic field induces circulating loops of current in it, called eddy currents due to electromagnetic induction. The loops flow perpendicular to the magnetic field axis. The energy of the currents is dissipated as heat in the resistance of the core material. The power loss is proportional to the area of the loops and inversely proportional to the resistivity of the core material. Eddy current losses is reduced by making the core out of thin laminations which have an insulating coating, or alternately, making the core of a nonconductive magnetic material, like ferrites. Deji A. (2011) and Deji A. (2016)

Anomalous losses

By definition, this category includes any losses in addition to eddy-current and hysteresis losses. This can also be described as broadening of the hysteresis loop with frequency. Physical mechanisms for anomalous loss include localized eddy-current effects near moving core in the inward and outward domain geometry. Having carefully taken care of these losses, the circuit is applied for testing.

Application and Implementation

One of the eminent applications of the designed differential inductive sensor is for sensing the speed motion, gear tooth sensing, cam-crankshaft sensing and sensing of metal objects in human body. One easy way of attaining this is to fabricate a chip having the whole novel concept in the inward and outward motion due to oscillation providing the practical capability of sensing /detecting the metallic deposit even inside the human body after war, or even other health issue like kidney stone and respiratory derogation. The future concept of the differential sensing architecture in chip is shown in Figure 8 (a) and (b).
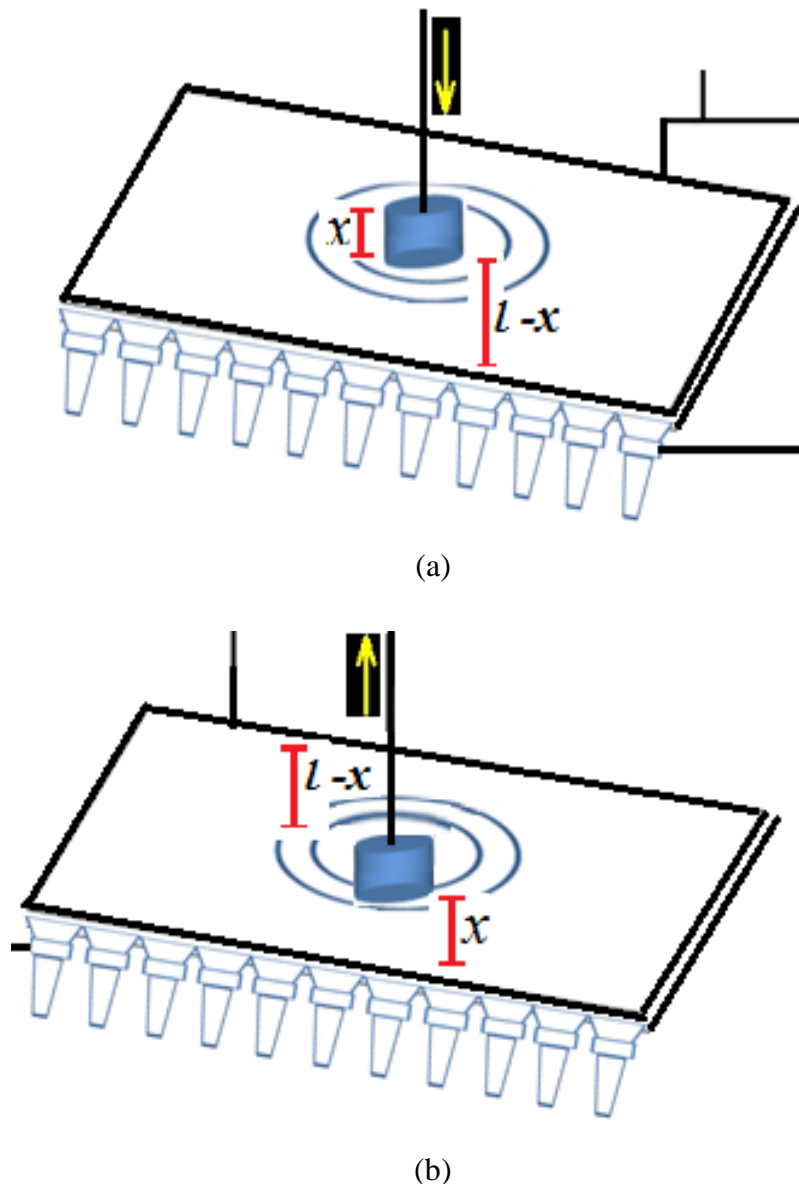
(a)

(b)

Figure 4: (a) Differential core moving into a coil due to vibrations (b) Differential core moving out of the coil due to vibrations

7.1 Applying the Differential position to an Industrial Machine

When the differential position sensor is applied to industrial machine made with spring, the vibration and oscillation from the machine, result in producing continuous oscillation, thereby producing the force/pressure necessary for generating frequency, voltage, current, duty cycle and other useful signal. The results obtained shows the voltage output from the industrial machine tested. This means that the target vibrations are converted into useful current and voltage for electrical application. This applied differential mechanism is shown in Figure 9. The result from Figure 9 is shown in Figure 10.

From Figure 10, it is shown or seen that as the machine vibration start initially, the output voltage produced has a two-step output meaning less voltage. As the vibration increases, more voltage in a short cycles per second are produced. This gives rise to higher frequency output as well. This application result is shown in Figure 10.
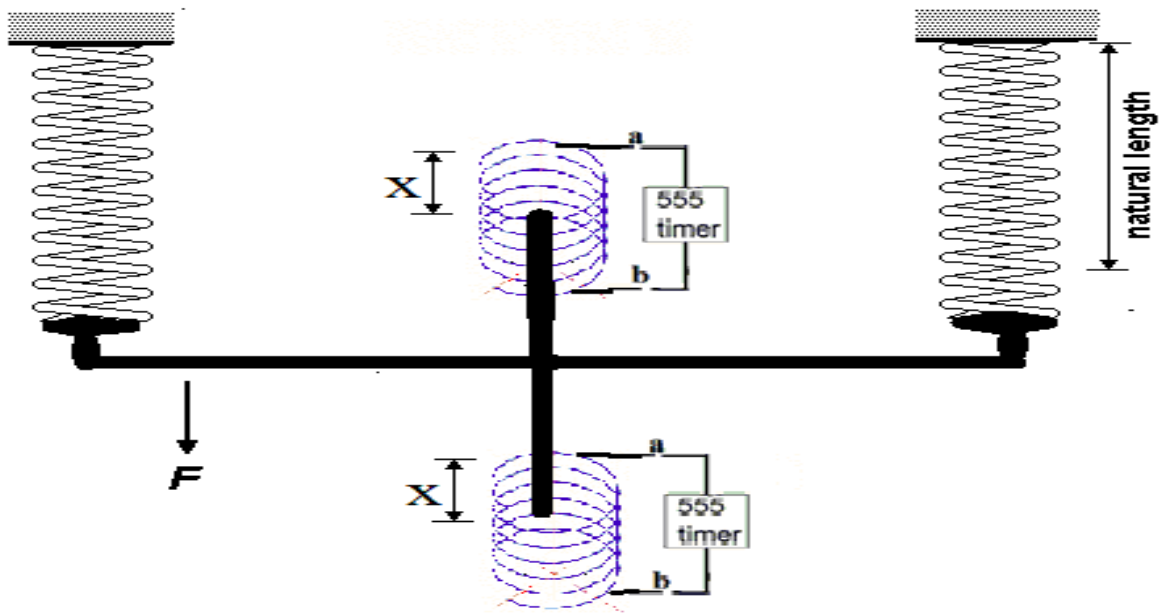
Figure 5: Signal produced from circuit oscillation and vibrations.

The timer circuit when connected to the coils in Figure 9 will give rise to voltage in Figure 10. This RL3R circuit gives us a square wave with a frequency depending on the inductance value of the coil as shown in Figure 10.
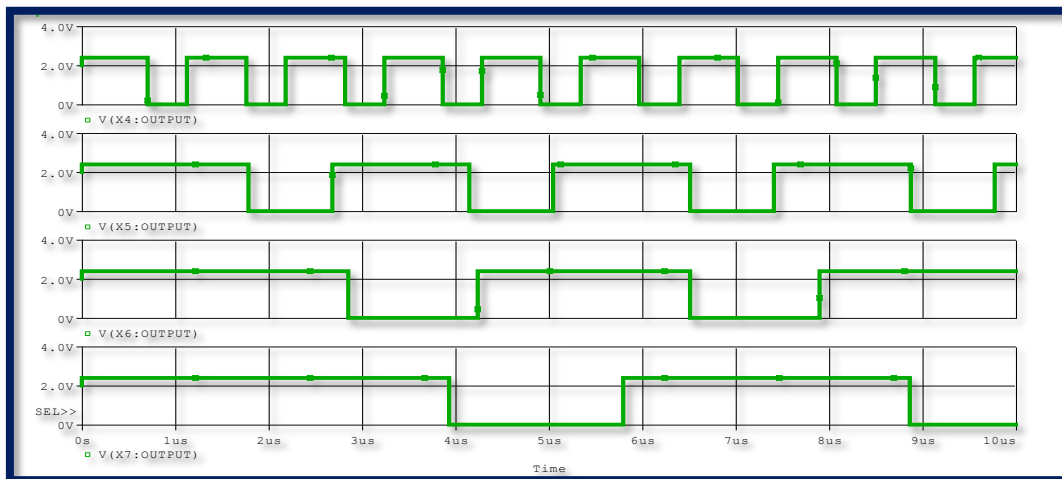

Figure 6: Voltage waveform from circuit Oscillation

7.2 Applying the Differential position to Human body

The above circuit when fabricated on a chip can be fitted to a pacemaker for being applied to verify the body conditions under intense situation. In this case, the change in inductance of the coil as a function of the movement of the core respond to ambient body environment by translating the differential deviations from the sensor whose pressure or net force comes from the heart beat. This translates this implantable medical device (IMD) into signal generator. The frequency and voltage output can be modulated into a pulse stream via gatherable protocols, the application scenarios. This IMD can also be used in detecting medical anomalies in the bodies' especially metallic deposit in the body (Ezzat 2011, Ezzat 2012,

Mohammed 2012, and Ferran 2009, Sheroz 2012) and Deji 2010, Deji 2011, Deji 2012, Deji 2014, Deji 2016 Deji 2023 and Deji 2023). The mechanism of operation is stated below;

The iron core is inserted 6mm into the coil. The value of frequency is recorded. The core is again inserted into 12mm and then followed by 18mm, 24mm, 30mm, and 36mm respectively. When the core is fully inserted into coil, the value of the frequency is recorded. Then, the core is being pulled in 6mm steps passing over values of 6mm followed by 12mm, 18mm, 24mm, 30mm, and 36mm respectively.

When the core is being pulled out completely from the coil, the value of frequency is recorded. The above procedure is repeated three times for calculating the final results at average values. Subsequently, the same procedure is performed with core being replaced by nickel and copper, while recording the results for obtaining the result plots.

The characteristic performance of the designed differential sensory position sensor using inductive mechanism when compared with the recently reported sensor as the bench marked areas is shown significantly in table 7 This table gives each sensor performance characteristics and optimization, thereby giving us another edge or another area of notable contribution in terms of sensitivity, linearity and hysteresis.

Table 7: Comparison of Sensor characteristics [Deji 2012]

Sensor Type	Sensitivity	Linearity	Pre. Hyst	Tempt. Hyst
Piezor.p.s	25mV/kPa	Linear	±1% FSO	±2% FSO
Cap. Pre. Sensor	0.2nF/kPa	Nonlinear	±0.1% FSO	±0.5% FSO
LVDT	400mV/kPa	Linear	±0.5% FSO	±0.1% FSO
New Sensor	3.56mH/kPa	Linear	±0.05% FSO	±0.1% FSO
Newest Sensor	3.72mH/kPa	Highly Linear	±0.03% FSO	±0.1% FSO

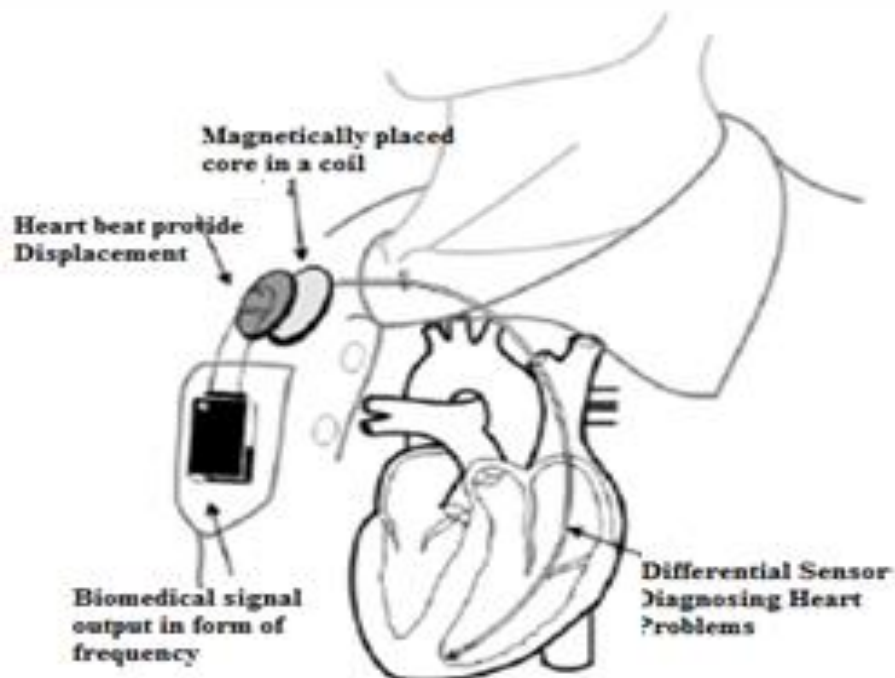The developed prototype is applied in human body as shown in Figure 11

Figure 7: Device applied to the respiratory and circulatory systems

This device comprises of coils of micro-dimensions in a core interfaced with a timer in an oscillator mode. The heartbeat provides the pressure which displaces the core leading into changes in inductance produced as frequency or duty cycle output. This frequency is analyzed to show the significance of coil pressure sensor and its biomedical diagnostic applications.

Experimental Linearization of the Output Frequency Signal

As shown in Figure 12 (a) and (b), the inductive change of core (L core) opposes the inductive change of air (Lair). It is also shown at the theoretical derivations equation (1) and (2) that the total inductance of the system is the sum up of Lair and L core. When the core is at central position the two frequencies are equal in amplitude. It is also possible to indicate the direction the core has moved using the simulation technique.

The experimental graphs shown in Figure 12 (a), (b) and (c) for inductance and displacements measurements respectively, have been found to have very good linearity. Initially, the seesaw is balanced for a particular position of the core. When the seesaw is unbalanced, the output frequency for different values of inductive coil displacement is measured in both increasing and decreasing modes. The variation of the unbalanced output with the change in core displacement are found to be linear. For all the graph shown in the above, the slope of the finding is $\mu_o N^2 A/l$. The theoretical plot and simulation is found out to be linearly related and both results demonstrated in the experiment.
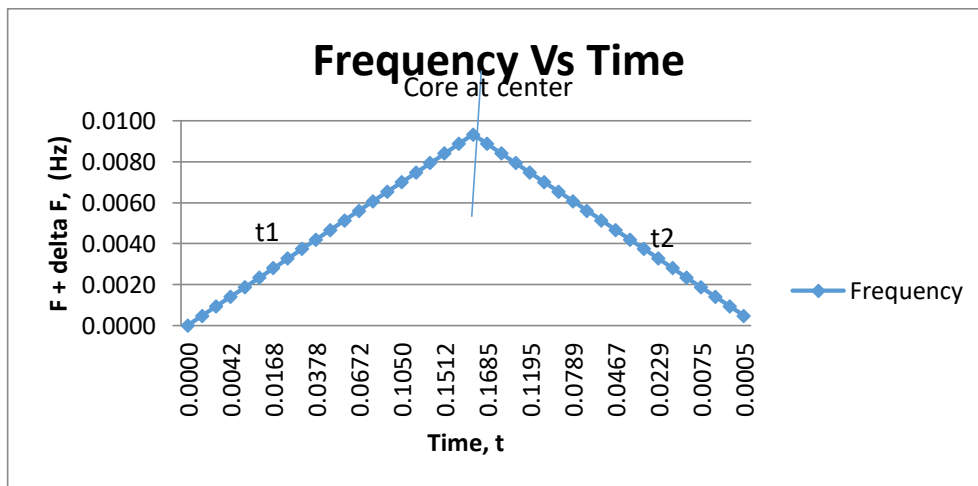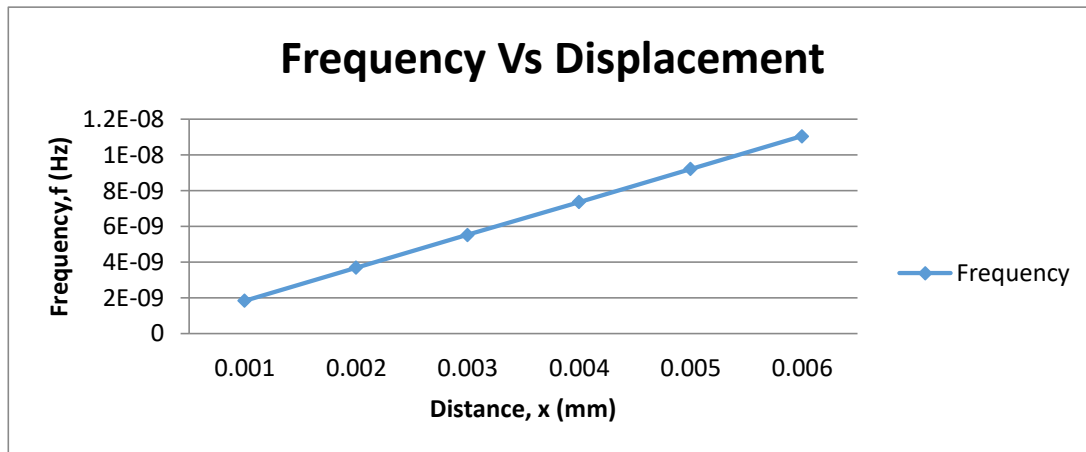

(a)
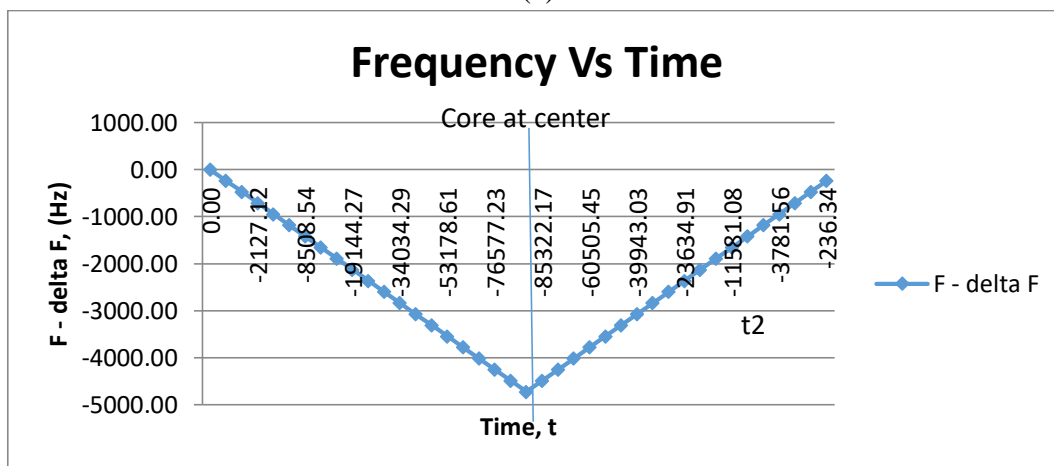
(b)

Figure 12: (a) Core is being pulled out of the coil (b) The core is moving into the coil (c) Linearized Frequency against Displacement

Error and Compensation Methods

The errors from the previous work is shown and that from this work for calculated and measured are shown Figure 6.16. A comparison between the results shows that less error is found in this case than in the previously reported work with a 0.01% reduction in value.

The errors from calculated and measured values are compensated by equation 3. And shown in Figure 13.

$$\sum_{x=0}^{x=l} 0.63 \frac{\mu_0 N^2 A}{Rl^2} \left(l + x(\mu_r - 1) \right) \tag{3}$$
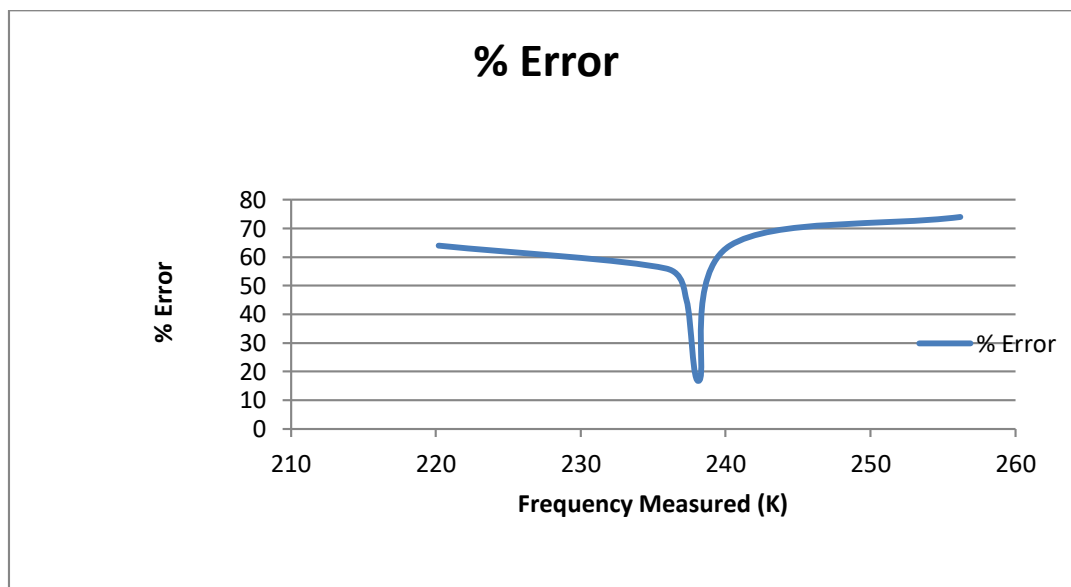

Figure 13: Percentage error in the measured value of the frequency

Conclusion

Experimentation of a differential sensing system is carried out so as to bridge the gap between numerous theoretical reports on sensor with circuit actualization. This design consists of two coils with varying cores in which a change in the core position will result in inductance change. These seeming variations are converted into frequency output in the processing part of the sensor using a timer circuit. Finally, this design provides a device for changing both biomedical stimuli and electromechanical system deviation in

form of nervous damage, sickness, oscillation, vibration to be harvested into useful electrical signal by the help of designed differential inductive sensor using both coils in a transducers as shown in Figure 1 (a), (b) and Figure 2. The result obtained verifies the derivations and the simulation in literature. The error is compensated with equation (3) brought to minima value of 0.01% of FSO.

This article describes a circuit which is used to convert inductance changes as a result of convulsion bar movement to frequency. The results are obtained from its application for acquisition of biomedical signal from a human body using an interface circuit properly designed for use with differential pressure sensors. In the result section, the importance of this circuit is illustrated by its error of 0.001% of the Full Scale Operation (FSO) as shown in Table 7. The sensitivity obtained in our case is much higher than reported one in the literature and with a 0.001FSO improvement.

Other notable contributions or value added to knowledge are:
- Frequency hysteresis from the inward and outward movement
- Kinematics of the oscillatory motion.
- Impedance voltage and its characteristics.
- Resonant frequency for the model and magnetic field generated as such.
- Spring application providing same oscillation.

References

1. Deji, A., Khan, S., Habaebi, H.M., Musa. O.S. (2024). Technical Engineering Evaluations and Economic Feasibility Study of Solar Powered Air Conditioning System in Tier Three Nations. *Academy of Entrepreneurship Journal, 30*(S1), 1-18.

2. Deji A., Sheroz K., Musse M.A., (December 2023) "*Analytical Modeling of Electrical Frequency and Voltage Signal from a Differential Inductive Transduction for Energy Measurement.* International Journal for Multidisciplinary Research. Volume 5 Issue 6 Page 1-19. **DOI:** 10.36948/ijfmr.2023.v05i06.8292

3. Deji A., Sheroz K., Musse M.A., (December 2023) "*Kinematic Motion Modelling from Differential Inductive Oscillation Sensing for a Sevomechanism and Electromechanical Devices and Applications.* International Journal for Multidisciplinary Research. Volume 5 Issue 6 Page 1-15. **DOI:** 10.36948/ijfmr.2023.v05i06.8291

4. Deji A., Hanifah A.M., Sherifah O.M., (December 2023) "*The Adoption of Information System Technology in Piloting the Current State of Health Institution in Tier Three Nations.*" International Journal for Multidisciplinary Research. Volume 5 Issue 6 Page 1-13. **DOI:** 10.36948/ijfmr.2023.v05i06.8367

5. Ezzat, G.B. and H.M. Marvin Cheng, AUGUST 2011. *"High-Sensitivity Inductive Pressure Sensor,"* *IEEE Transactions on Instrumentation And Measurement,* 60(8)

6. D. Abdulwahab et al., "Identification of linearized regions of non-linear transducers responses," International Conference on Computer and Communication Engineering (ICCCE'10), Kuala Lumpur, 2010, pp. 1-4, doi: 10.1109/ICCCE.2010.5556753.

7. D. Abdulwahab, S. Khan, J. Chebil and A. H. M. Z. Alam, "Symmetrical analysis and evaluation of Differential Resistive Sensor output with GSM/GPRS network," 2011 4th International Conference on Mechatronics (ICOM), Kuala Lumpur, Malaysia, 2011, pp. 1-6, doi: 10.1109/ICOM.2011.5937149.

8. Khan S., A. Deji, A.H.M Zahirul, J. Chebil, M.M Shobani, A.M Noreha. (Setember 2012) "Design of a Differential Sensor Circuit for Biomedical Implant Applications". *Australia. Journal of Basic and Applied. Sciences., 6(9): 1-9.* 10.1002/9781118329481.ch1.

9. Deji A., Sheroz K, Musse M.A, Jalel C. (August 2014). Analysis and evaluation of differential inductive transducers for transforming physical parameters into usable output frequency signal August 2014 International Journal of the Physical Sciences 9(15):339-349. DOI:10.5897/IJPS12.655

10. Deji A., Sheroz K, Musse M.A, Jalel C. (2011). Design of Differential Resistive Measuring System and its applications. A book chapter in IIUMPRESS on Principle of Transducer Devices and Components. Chapter 17, page 107.

11. Abdulwahab, Deji. *Development of Differential Sensor Interface for GSM Communication*. Kulliyyah of Engineering, International Islamic University Malaysia, 2011.

12. Abdulwahab Deji. *Development of Differential Inductive Transducer System for Accurate Position Measurement*. Kulliyyah of Engineering, International Islamic University Malaysia, 2016 Practical EE Copyright 2019). www.eepractical.com

13. Deji A., Sherifah OM., 2023. *The Mediating Effect of Entrepreneur Cash Waqf Intension as means of Planned Behaviour for Business Growth. International Journal for Multidisciplinary Research. Volume 5, Issues 6, page 1-22*

14. Elfaki Ahamed, O.M.H., Musa O.S, Deji A., (2023). Factors Related to Financial Stress Among Muslim Students in Malaysia: A Case Study of Sudanese Students. Academy of Entrepreneurship Journal, 29(6), 1- 15.

15. Mohammed, S. S, George A. B., Vanajakshi L., and Venkatraman J., (2012). "A Multiple Inductive Loop Vehicle Detection System for Heterogeneous and Lane-Less Traffic," IEEE Transactions on Instrumentation and Measurement, Vol. 61, No. 5, 1353-1361.

16. Ferran R., and Oscar C., (October 2009). Interfacing Differential Resistive Sensor to Microcontrollers: A Direct Approach. IEEE Trans. on Instrumentation and Measurement, Vol.58, No.10: 3405-3410.

17. Ezzat, G.B. and H.M. Marvin Cheng, AUGUST 2012. *"High-Sensitivity Inductive Pressure Sensor," IEEE Transactions on Instrumentation And Measurement,* 60(8).